Published in final edited form as:
Neuron. 2011 September 8; 71(5): 845–857. doi:10.1016/j.neuron.2011.06.038.

DEG/ENaC but not TRP channels are the major mechanoelectrical transduction channels in a *C. elegans* nociceptor

Shana L. Geffeney[1], **Juan G. Cueva**[1,*], **Dominique A. Glauser**[1,*], **Joseph C. Doll**[2], **Tim Hau-Chen Lee**[1,4], **Misty Montoya**[1], **Snetu Karania**[1], **Arman M. Garakani**[3], **Beth L. Pruitt**[2], and **Miriam B. Goodman**[†,1]

[1]Department of Molecular and Cellular Physiology, Stanford University, Stanford, CA 94305 USA

[2]Department of Mechanical Engineering, Stanford University, Stanford, CA 94305 USA

[3]Reify Corporation, Saratoga, CA 95070 USA

Summary

Many nociceptors detect mechanical cues, but the ion channels responsible for mechanotransduction in these sensory neurons remain obscure. Using *in vivo* recordings and genetic dissection, we identified the DEG/ENaC protein, DEG-1, as the major mechanotransduction channel in ASH, a polymodal nociceptor in *Caenorhabditis elegans*. But, DEG-1 is not the only mechanotransduction channel in ASH: loss of *deg-1* revealed a minor current whose properties differ from those expected of DEG/ENaC channels. This current was independent of two TRPV channels expressed in ASH. Although loss of these TRPV channels inhibits behavioral responses to noxious stimuli, we found that both mechanoreceptor currents and potentials were essentially wild-type in TRPV mutants. We propose that ASH nociceptors rely on two genetically-distinct mechanotransduction channels and that TRPV channels contribute to encoding and transmitting information. Because mammalian and insect nociceptors also co-express DEG/ENaCs and TRPVs, the cellular functions elaborated here for these ion channels may be conserved.

Introduction

Intense mechanical stimuli activate specialized sensory neurons (nociceptors) embedded in the skin and trigger withdrawal responses. Such behavioral responses protect animals from damage and in humans the activation of nociceptors is usually perceived as pain. Such perceptions rely on a multi-step process in which sensory neurons detect mechanical loads and transmit this information as electrical signals. Work in a variety of model organisms has identified genes encoding ion channels critical for the ability to sense both noxious and gentle touch. Among these genes are several members of the *trp* (transient receptor potential or TRP) and *deg/ENaC* (degenerin/epithelial Na^+ channel or DEG/ENaC) ion channel gene

[†]Correspondence to: Miriam B. Goodman, B-111 Beckman Center, 279 Campus Dr, Stanford, CA 94305, mbgoodman@stanford.edu, tel: 650-721-5976, FAX: 650-725-8021.
[*]Authors Contributed Equally
[4]Present Address: University at Buffalo School of Medicine and Biomedical Sciences, Buffalo, New York, USA

families (Arnadóttir and Chalfie, 2010; Basbaum et al., 2009; Lumpkin et al., 2010). Because they encode ion channel subunits, they are excellent candidates to form mechano-electrical transduction (MeT) channels essential for transforming mechanical stimuli into electrical signals. The ion channel proteins essential to form MeT channels are defined only for the gentle touch receptor neurons PLMs (O'Hagan et al., 2005) and for the cephalic CEP neurons (Kang et al., 2010) in *C. elegans*. MeT channels are formed by DEG/ENaC proteins in PLMs and TRP proteins in CEPs. The ion channel proteins that form MeT channels that detect mechanical cues in nociceptors have yet to be determined.

Many nociceptors, including those forming mammalian C fibers, express both DEG/ENaC and TRP channels proteins (Lumpkin and Caterina, 2007; Woolf and Ma, 2007). Notable examples include multidendritic neurons in *Drosophila* larvae (Tracey et al., 2003; Zhong et al., 2010) and in *C. elegans* (Chatzigeorgiou and Schafer, 2011; Chatzigeorgiou et al., 2010). Some studies suggest that both channel types are needed for responses to mechanical cues, while others have demonstrated that only one of these channel types has a role. In *Drosophila* larvae both the Pickpocket DEG/ENaC channel and the Painless TRP channel are required in multidendritic neurons for behavioral responses to noxious mechanical stimuli (Tracey et al., 2003; Zhong et al., 2010). Because optogenetic stimulation of these neurons evokes aversive behaviors in larvae lacking Pickpocket, Zhong et al. (2010) proposed that Pickpocket is upstream of Painless in the mechanosensory signalling pathway. In *C. elegans*, by contrast, only DEG/ENaC channels are required for noxious mechanical stimulus-evoked calcium transients in the PVD and FLP multidendritic neurons (Chatzigeorgiou and Schafer, 2011; Chatzigeorgiou et al., 2010). Indeed, mechanoreceptor currents (MRCs) in PVD have properties expected of currents carried by DEG/ENaC channels (Li et al., 2011).

Like the multidendritic neurons, the amphid ASH neurons in *C. elegans* also co-express DEG/ENaC and TRP channels. For several reasons, these neurons are an excellent model nociceptor. First, they are polymodal: chemical, osmotic and mechanical stimuli evoke transient increases in cytoplasmic calcium and an ASH-dependent withdrawal behavior (Chronis et al., 2007; Hilliard et al., 2005; Kindt et al., 2007). An intact ASH is required for full sensitivity to multiple aversive stimuli (Hart et al., 1995; Kaplan and Horvitz, 1993). Second, artificial activation of the ASH neurons is sufficient to induce defensive avoidance behavior (Guo et al., 2009; Tobin et al., 2002). Thus, ASH neurons perform all of the functions expected of a polymodal nociceptor. The ASH neurons express at least two *deg/ENaC* and two *trp* genes (Colbert et al., 1997; Hall et al., 1997; Tavernarakis et al., 1997; Tobin et al., 2002): the *deg/ENaC* genes are *deg-1* and *unc-8* which encode proteins related to the MEC-4 and MEC-10 proteins that form force-gated ion channels in *C. elegans* touch receptor neurons, while the *trp* channel genes are *osm-9* and *ocr-2* both of which encode TRPV proteins. Until now, the lack of deletion alleles in *deg-1* and *unc-8* has limited understanding of their role in ASH. In contrast, a great deal is known about the TRPV channel genes *osm-9* and *ocr-2*. Both genes are required to induce a behavioral response (Colbert et al., 1997; Tobin et al., 2002) and *osm-9* is needed to induce calcium transients to multiple noxious stimuli (Hilliard et al., 2005). (The contribution of *ocr-2* to nose touch-evoked calcium transients has not been tested.) These data and the recent demonstration that optogenetic stimulation of ASH works in *osm-9* mutants (Guo et al., 2009) support the proposal that OSM-9 is a candidate subunit of an MeT in ASH (Colbert et al., 1997; Hilliard et al., 2005; Tobin et al., 2002).

In this study, we combined *in vivo* whole-cell patch-clamp recording and genetic dissection to deconstruct mechanoreceptor currents (MRCs) in ASH neurons. The force required to activate ASH is two orders of magnitude larger than that required for activation of the PLM gentle touch receptor neurons (O'Hagan et al., 2005). MRCs in ASH are both Na^+-dependent

and inhibited by amiloride, properities of DEG/ENaC channels. Indeed, the major component of MRCs in ASH nociceptors was dependent on *deg-1*, a gene that encodes a DEG/ENaC channel subunit. Deleting DEG-1, uncovered a second, minor current that was *deg-1*-independent and had the same activation kinetics as the total current, but a distinct current-voltage relationship indicating that it is not carried by a DEG/ENaC channel. This minor current was also independent of *osm-9* and *ocr-2*, since MRCs were similar in *deg-1* single mutants and *osm-9ocr-2;deg-1* triple mutants. Both TRPV proteins were also dispensable for the major component since MRCs were essentially wild type in *osm-9* and *ocr-2* single mutants as well as in *osm-9ocr-2* double mutants. Additionally, mechanoreceptor potentials (MRPs) evoked by saturating stimuli were likewise unaffected by the loss of OSM-9 and OCR-2. These data suggest that TRPV channels have a critical role in later steps of sensory perception: encoding and transmission of sensory information, but not in detection.

Results

Wild-type Mechanoreceptor Currents in ASH neurons

We used a slit-worm preparation and *in vivo* whole-cell patch clamp recording (Goodman et al., 1998) to measure electrical responses to mechanical stimulation in ASH nociceptor neurons. To unambiguously identify ASH in both wild type and mutant animals, we expressed green fluorescent protein (GFP) under the control of an ASH-selective promoter (Experimental Procedures). Using this label also allowed us to determine that the sensory ending of ASH remained intact after the cell body was exposed for patch-clamp recording. These sensory endings innervate structures next to the mouth of the animal called amphids. We applied mechanical stimuli to ASH by compressing the entire “nose” of the animal (Figure 1A), an area defined as the buccal cavity and surrounding sensory structures.

We found that compressing the nose of immobilized *C. elegans* nematodes activates an inward MRC in wild-type ASH neurons. This current rises rapidly and decays during force application (Figure 1). In some, but not all recordings, we also observed channel activation at the offset of mechanical stimulation (Figure 1C). Such off-responses may be a shared feature of nonauditory mechanoreceptors since they have been observed in three other mechanoreceptor neurons in *C. elegans* (Kang et al., 2010; Li et al., 2011; O'Hagan et al., 2005) as well as in cultured dorsal root ganglion neurons (Poole et al., 2011).

As reported for other *C. elegans* mechanoreceptors (Kang et al., 2010; O'Hagan et al., 2005), MRCs decay during force application suggesting that either the channels carrying this current or the protein machinery that transfers force to them adapts to sustained force over time. In addition to this rapidly-activating current, we found evidence of additional currents that activated following a delay of tens of milliseconds in some recordings (Figure S1). The origin of such currents is unknown and we were unable to study them since their size declined with repeated stimulation. In this study, we focused on responses to mechanical stimulation that contained only the initial, rapidly activating MRC.

We quantified activation and decay rates by fitting MRCs with a modified alpha function (Figure 1B, thick aqua line), as described (O'Hagan et al., 2005). On average, the time constant for MRC activation in wild-type ASH neurons was ~3 ms while the time constant for decay was ten-fold longer or ~30 ms (Table 1). Both the activation and decay rates (τ_1 and τ_2, respectively) are indistinguishable from those reported previously for MRCs in PLM neurons (O'Hagan et al., 2005), while activation rates are slower than those found in CEP neurons (Kang et al., 2010). (The decay rate for MRCs in CEP has not been reported.)

We found that larger forces were required to activate MRCs in ASH than in the gentle touch receptor neuron PLM (O'Hagan et al., 2005). The amplitude of MRCs increased with stimulus strength (Figure 1D) and plotting their amplitude *versus* force across multiple recordings shows that the half-activation force is ~11 μN in ASH (Figure 1E). This is two-orders of magnitude larger than the force required for half-maximal responses in PLM. These data provide further evidence that ASH is functioning as a nociceptor in *C. elegans*.

The latency between stimulus delivery and channel activation was measured as described (O'Hagan et al., 2005) and had an average value of 3.4 ms (Table 1). This time encompasses several events, including the time needed to move the probe in contact with the animal, transmit force from the cuticle to MeT channels and the time needed to activate them. While it is not possible to directly measure all of these time intervals, we can estimate the time required to move the probe from its starting position into contact with the nose from the probe's intrinsic resonant frequency and the quality of such resonance. Using interferometry, we measured the resonant frequency of one of our force probes in air and used this value to derive an estimate of its resonant frequency and quality in saline: F_o = 130 Hz, and quality factor, Q = 7 (see Experimental Procedures). From these parameters, we estimate that the time required to move the probe is 1.3 ms. Thus, the latency for channel activation is 2.1 ms or less. This latency is longer than the shortest latencies measured for other *C. elegans* neurons (O'Hagan et al., 2005; Kang et al., 2010), but, because the fastest known second messenger-based sensory transduction pathway has a latency of 20 ms (Hardie, 2001), we propose that this latency is brief enough to suggest that force acts directly on the MeT channels that carry MRCs in ASH.

Sinusoidal oscillations were detected in many of our MRC recordings suggesting that channel activation is able to follow the rapid, resonant movements of the probe (Figure 1B). To determine the frequency of MRC oscillations we fit the total MRC with an alpha function and subtracted this fit from the average current to isolate the sinusoidal variations in current (Figure 1B) . In five recordings with high-quality oscillations, the MRC oscillation frequency had an average value of 130 ± 6 Hz (mean ± s.e.m., n = 5). Thus, channels carrying MRCs in the ASH neurons can follow rapid variations in applied mechanical loads.

MRCs Are Blocked by Amiloride and Carried Primarily by Na^+ Ions

Mechanoreceptor currents, if mediated by a DEG/ENaC channel complex, should be carried by Na^+ ions and blocked by amiloride. Conversely, if MRCs were carried by a TRPV channel complex, they should be permeable to both Na^+ and K^+ and resistant to amiloride. Wild type MRCs were reversibly blocked by amiloride (Figure 2A, 2B). The fraction of peak current blocked by 300 μM amiloride was 0.77 ± 0.06 (n = 4) and 0.75 ± 0.10 (n = 3) at −90 and −60 mV, respectively. This same level of MRC block was achieved in the gentle touch receptor neuron PLM that expresses the DEG/ENaC channel subunits MEC-4 and MEC-10 with 200 μM amiloride (O'Hagan et al., 2005). MRCs in ASH maybe carried by DEG/ENaC channels that are more resistant to amiloride than MEC-4 and MEC-10 or ASH may express a distinct population of channels that is insensitive to amiloride. Below we provide evidence that MRCs are carried by two classes of ion channels.

The ASH neurons terminate in a single cilium that extends into the external environment through an opening n the amphid (Perkins et al., 1986). If the MeT channels localize to this cilium, then exogenous amiloride should inhibit behavioral responses to nose touch. Consistent with this prediction, animals exposed to amiloride for more than 30 minutes showed a modest, but statistically significant decrease in sensitivity to nose touch (Figure 2C). Such a minor effect on nose touch sensitivity is the expected result for two reasons. First, 300μM amiloride does not completely block MRCs (Figure 2A, 2B). Second, ASH is not the only mechanoreceptor neuron responsible for sensitivity to nose touch (Kaplan and

Horvitz, 1993), but it is the only one exposed to the external environment. Laser ablation studies have demonstrated that animals where only ASH is killed are more likely to respond to nose touch stimuli than animals where all nose touch receptor neurons have been killed (Kaplan and Horvitz, 1993). Thus, even a complete block of MRCs in ASH would produce only a partial inhibition of behavioral responses to nose touch.

We then examined whether MRCs were Na^+-dependent. The reversal potential for Na^+ ions in our solutions was +40 mV. Wild-type MRCs were inward across a wide range of membrane potentials (Figure 2F, Figure 4E). In control saline, inward rectification was sufficiently strong that outward currents could not be detected, even at voltages as high as +80 mV (Figure 4E). The ionic basis of such strong inward rectification is not known, but could reflect multiple factors including high calcium permeability and voltage-dependent block of outward current. Replacing extracellular Na^+ with a large, monovalent cation (*N*-methyl-*D*-glucamine) dramatically decreased inward MRCs at −60 mV (Figure 2D, 2E), shifted the reversal potential of the peak MRC to −47 mV and increased outward currents (Figure 2F). This last effect could reflect relief of inhibition by extracellular Na^+ ions as reported for ENaC channels (Bize and Horisberger, 2007). On average, MRCs reversed polarity at −51 ± 5 mV (mean ± s.e.m, $n = 4$) in Na^+-free saline. These effects indicate that MRCs are Na^+-dependent in control saline and suggest the most of the channels that carry such currents are Na^+-permeable.

Wild-type *deg-1*, but not *unc-8* Is Required for MRCs *In Vivo*

The ASH neurons express at least two members of the DEG/ENaC gene family: *deg-1* and *unc-8* (Hall et al., 1997; Tavernarakis et al., 1997). We investigated the effect of large deletions in *deg-1* and *unc-8* on the generation of MRCs in the ASH neurons. Deleting *unc-8* had no effect on the generation of force-activated MRCs (Figure 3A, Table 1). By contrast, loss of *deg-1* reduced MRCs by 80% and MRCs in *unc-8;deg-1* double null mutants were similar to those in *deg-1* single mutants (Figure 3A, Table 1). None of these mutations affected voltage-activated currents in ASH thus the effects of the mutations in *deg-1* are limited to MRCs (Figure 3B, 3C). In addition to reducing current size, loss of *deg-1* shifted the reversal potential of the peak MRCs to −23 ± 5 mV (Figure 5B). These results suggest that the ion channels responsible for the *deg-1*-independent currents are not primarily sodium-permeable and are unlikely to be formed by the remaining UNC-8 protein. Instead, they appear to be permeable to potassium and sodium, a property of TRPV channels.

Thus, *deg-1*, but not *unc-8*, is essential for the major component of MRCs in ASH. We note that while *unc-8* is not required for the generation of MRCs in ASH, it remains possible that MeT channels contain both DEG-1 and UNC-8. If this scenario is correct, then our data imply that DEG-1 forms functional channels in the absence of UNC-8, but that UNC-8 is unable to function without DEG-1. A similar situation exists in *C. elegans* touch receptor neurons in which MEC-4 functions in the absence of MEC-10, but not *vice versa* (O'Hagan, 2005).

Having established the essential role of DEG-1, next we sought to determine how missense mutations in the DEG-1 protein affect MRCs by recording from *deg-1(u506u679)* mutants. This mutant allele was recovered in a screen for suppressors of *deg-1(u506)*-induced necrotic cell death and encodes two point mutations (García-Añoveros et al., 1995): an alanine to threonine change in the extracellular domain (A393T) that causes cell death when present alone and a glycine to arginine change in the conserved second transmembrane domain (G710R) that suppresses the A393T-induced cell death. We chose to study this allele because a change in the equivalent glycine residue of MEC-4(G716D) or MEC-10(G676R) alters the reversal potential and ion selectivity of MRCs recorded in PLM neurons (Figure 4A, O'Hagan et al., 2005). If DEG-1 is a pore forming subunit of the MeT

channel then the G710R mutation should shift the reversal potential of MRCs in ASH. We tested this prediction by recording MRCs in *deg-1(u506u679)*.

Mechanoreceptor currents in *u506u679* mutants were smaller than in wild type (Figures 4B, C), but larger than in *deg-1* deletion mutants (Table 1), suggesting that this allele is not null. Nevertheless, the effect of *u506u679* on MRC amplitude is sufficient to induce a modest decrease in the ability of animals to respond to nose touch (Figure 4D). Unlike wild type MRCs, which have an estimated reversal potential of more than +100 mV in control saline, *u506u679* MRCs reverse polarity near 0 mV (Figure 4E). Thus, *u506u679* alters the ion selectivity of MRCs *in vivo*. We note that the reversal potential of this mutant is different than that measured for *deg-1* null mutants, supporting the idea that *u506u679* not a null allele of *deg-1*. We do not know whether the effect of *u506u679* on ion selectivity is due to the extracellular A393T mutation, the G710R mutation in the second transmembrane domain, or both. However, since the G710R mutation in DEG-1 affects the residue equivalent to the one mutated in *mec-4(u2)* [G716D] and *mec-10(u20)* [G676R] that alters the reversal potential of MRCs in PLM, it seems likely that this point mutation accounts for the change in selectivity. Regardless of whether the change in selectivity depends on one or both point mutations, this finding demonstrates DEG-1 is a pore-forming subunit of a channel that is critical for generating mechanoreceptor currents in ASH.

Loss of OSM-9, OCR-2 or Both Proteins Has No Effect on MRCs

The *osm-9* and *ocr-2* genes encode TRPV channel proteins co-expressed in ASH and required for ASH mediated responses to noxious physical and chemical stimuli (Colbert et al., 1997; Tobin et al., 2002). Loss of *osm-9* inhibits nose touch-evoked calcium transients in ASH (Hilliard et al., 2005), supporting the idea that TRPV proteins form sensory mechanotransduction channels in ASH and elsewhere. Until now, this idea has not been tested directly. We recorded from ASH neurons in animals carrying null mutations in *ocr-2*, *osm-9* or in *osm-9ocr-2* double null mutants. We found that MRCs were retained in all three mutant genotypes (Figure 5A, Table 1), indicating that neither TRPV protein is required for the generation of MRCs. Additionally, loss of one or both of these ASH-expressed TRPV channels had no detectable effect on the size, latency, or time course of MRCs (Table 1). Furthermore, though TRPV null mutations shifted the MRC current-voltage relationship toward 0 mV, MRCs reversed above +40 mV. Thus, the major component of MRCs in TRPV mutants remains a Na^+-permeable channel indicating that neither TRPV channel is a major contributor to MRCs in ASH (Figure 5B, 5C). Next, we determined how loss of *ocr-2* and *osm-9* affected the minor *deg-1*-independent MRC and found that MRCs in *osm-9ocr-2*;*deg-1* triple mutants were the same size and had the same kinetics as *deg-1* single mutants (Figure 5A, Table 1). The triple mutant also had same reversal potential as *deg-1* mutants (Figure 5B). Collectively, these data establish that neither the major or minor components of mechanotransduction current in ASH require OSM-9 or OCR-2.

OSM-9 and OCR-2 Are Not Required for the Generation of MRPs

Force depolarized ASH neurons as expected for changes in membrane potential activated by inward currents (Figure 5D). The MRP time course reflected that of the underlying MRC. No action potential-like events were detected either in response to force or current injection (Figure S2). Thus, like other sensory neurons in *C. elegans* (Goodman et al., 1998; O'Hagan et al., 2005; Ramot et al., 2008), the ASH neurons appear to signal without using classical action potentials.

MRPs evoked by saturating mechanical stimuli were similar in wild type and *osm-9ocr-2* double mutant ASH neurons (Figure 5D, Table 2), reaching average maxima of −39 ± 3 mV (mean ± s.e.m., n=10) and −35 ± 2 mV (mean ± s.e.m., n=5), respectively (Table 2). Such

MRPs are likely to open voltage-gated calcium channels since depolarization above −50 mV is sufficient to activate calcium currents in other *C. elegans* sensory neurons (Goodman et al., 1998). Force evoked only tiny depolarizations in *deg-1* ASH neurons that never rose above −50 mV (Figure 5D, Table 2), suggesting that voltage-gated calcium channels are not activated in ASH neurons lacking DEG-1. In all genotypes studied, MRP amplitude mirrored MRC size (Figure 5D). These results demonstrate that OSM-9 and OCR-2 are not required for the generation of either MRPs or MRCs and establish that DEG-1, by contrast, is essential for the generation of both MRPs and MRCs.

Discussion

The eponymous *deg-1* was the first DEG/ENaC gene to be identified in any organism (Chalfie and Wolinsky, 1990). Here, we show that it encodes the third DEG/ENaC protein known to be a pore-forming subunit of a sensory MeT channel. Several lines of evidence support this conclusion. First, external loads open amiloride-sensitive, sodium-permeable ion channels in ASH. Because of the millisecond latency between stimulus delivery and channel activation, we propose that this channel is likely to be directly activated by mechanical loads. Second, loss of *deg-1* eliminates 80% of the total MRC. This is not due to a general defect caused by gene mutation, however, since loss of three other ASH-expressed ion channel genes, *unc-8*, *osm-9* and *ocr-2*, has no effect on MRCs. Additionally, *deg-1* mutants have no effect on voltage-activated currents in ASH. Finally, mutations that alter, but do not eliminate DEG-1 decrease MRC amplitude and modify MRC ion selectivity. This last finding is critical for two reasons. First, it demonstrates that DEG-1 is expressed in the ASH neurons, as initially reported (Hall et al., 1997), but recently contested (Wang et al., 2008). Second, and most critical for the present study, this finding establishes that DEG-1 is a pore-forming subunit of the primary channel responsible for allowing the ASH neurons to detect aversive mechanical stimuli.

In ASH Nociceptors, MRCs Are Carried by Two Classes of Ion Channels

Mechanoreceptor currents in ASH nociceptors share several features with those reported previously in other mechanoreceptor neurons in *C. elegans* (Kang et al., 2010; O'Hagan et al., 2005), spiders (Juusola et al., 1994), and certain dorsal root ganglion neurons studied *in vitro* (Drew et al., 2002; Hao and Delmas, 2010; Hu and Lewin, 2006; McCarter et al., 1999). One shared feature is the kinetics of MRCs: in all of these cell types, currents activate rapidly following stimulation, but decay during continued stimulation. Until now, it has been assumed that a single class of ion channels is responsible for MRCs in individual mechanoreceptor neurons since their activation and decay follow a single exponential time course.

Using genetic dissection and *in vivo* patch-clamp recording, we discovered that mechanoreceptor currents in ASH are composed of at least two distinct currents: the major *deg-1*-dependent current, which accounts for more than 80% of the peak amplitude and the minor *deg-1*-independent current that carries the rest. Our work contrasts with the results from other *C. elegans* neurons where the loss of a single channel subunit eliminated MRCs (Kang et al., 2010; O'Hagan et al., 2005) and is similar to findings from *Drosophila* bristle receptors in which the loss of NompC reduces MRCs by 90% (Walker et al., 2000). The major and minor currents in ASH differ in their reversal potential, suggesting that distinct classes of ion channels carry these currents. Although the molecular identity of the *deg-1*-independent channel is not yet known, we show that it is independent of both *osm-9* and *ocr-2*, since *osm-9ocr-2;deg-1* triple mutants have MRCs that are indistinguishable from those observed in *deg-1* single mutants. Candidates include non-selective cation channels such as the other 22 members of the TRP channel family in *C. elegans* (Glauser et al., 2011; Goodman and Schwarz, 2003) and the *C. elegans* ortholog of the Piezo proteins recently

shown to be required for generation of mechanically-activated currents in cultured dorsal root ganglion neurons (Coste et al., 2010).

Our data demonstrate that mechanoreceptor currents in ASH are carried by two genetically-separable currents but we do not know whether force activates these two currents in a sequential or parallel fashion. In any plausible sequential model, the minor current must be upstream of the major current because it remains when *deg-1* is lost and thus its activation must precede activation of the major current. But, the minor current does not activate faster than the total current. Also, if the major *deg-1*-dependent current were activated in response to the minor current, this event must be complete in milliseconds or less. Most second messenger systems are not that rapid. While we cannot eliminate the sequential model, we favor the parallel model and propose that ASH expresses two sensory mechanotransduction channel complexes, one of which uses DEG-1 as a pore-forming subunit. The use of multiple mechanotransduction channels may not be unique to ASH; other mechanoreceptor neurons may express multiple classes of mechanotransduction channels (Göpfert et al., 2006; Walker et al., 2000). This functional redundancy could account for difficulties in identifying a single channel type responsible for mechanoreceptor currents in mammalian somatosensory neurons, including nociceptors.

In Both Touch Receptors and Nociceptors, MRCs Are Carried by DEG/ENaC Channels

Most animals are endowed with a complex array of sensory neurons specialized to detect mechanical energy in the form of touch, vibration or body movements. Such neurons vary not only in the loads and strains they detect, but also in their sensitivity. In the present work and in a prior study (O'Hagan et al., 2005), we have shown that two kinds of *C. elegans* mechanoreceptor neurons, ASH and PLM neurons, respond to force using channels formed by DEG/ENaC proteins. The two kinds of neurons differ in their sensitivity to mechanical loads: nearly one hundred-fold higher forces are required to activate mechanoreceptor currents in ASH nociceptors (this study) than in the PLM touch receptor neurons (O'Hagan et al., 2005). The difference in sensitivity could reside in the MeT channels themselves. In this scenario, each DEG/ENaC subunit would harbor a force sensor that links mechanical loads to channel gating, but the sensors would vary in the forces required to activate them. Alternatively, the primary determinant of force sensitivity could be the cellular machinery that transmits loads from the body surface to the channel proteins embedded in the sensory neuron's plasma membrane. These two modes for establishing the exact force-dependence of MeT channels *in vivo* are not mutually exclusive, however. Regardless of the molecular and cellular basis for the difference in sensitivity, our work establishes that both low-threshold, gentle touch receptor neurons and high-threshold nociceptors rely on DEG/ENaC proteins to form amiloride-sensitive, sodium-permeable channels responsible for MRCs *in vivo*.

Wild-type MRPs Depend On DEG/ENaC Channels, But Not TRPV Channels

As expected from the force-dependent activation of Na^+-permeable, DEG-1-dependent channels, mechanical loads depolarize the ASH nociceptor. Unexpectedly, we found that the TRPV proteins OCR-2 and OSM-9 were not required for the generation of either mechanoreceptor currents or mechanoreceptor potentials. At first glance, this electrophysiological finding is difficult to reconcile with the essential role for both OCR-2 and OSM-9 in behavioral responses to nose touch (Colbert et al., 1997; Tobin et al., 2002) and the contribution of OSM-9 to nose touch-evoked somatic calcium transients (Hilliard et al., 2005). Insight into this paradox comes from the following observations. First, the FLP and OLQ neurons, which act in parallel with ASH to mediate avoidance of nose touch (Chatzigeorgiou and Schafer, 2011; Kaplan and Horvitz, 1993), also express OSM-9 (Colbert et al., 1997; Tobin et al., 2002). Thus, the strength of the behavioral phenotype

associated with null mutations in *osm-9* could reflect modest defects in signaling mediated not only by ASH, but also by FLP, and OLQ. Second, the requirement for OSM-9 in nose touch-evoked somatic calcium transients has been observed only in the presence of exogenous serotonin (Hilliard et al., 2005). Exogenous serotonin is not required for nose touch-induced calcium transients in ASH (Ezcurra et al., 2011; Kindt et al., 2007), but enhances ASH-mediated behavioral responses to nose touch in animals deprived of bacterial food (Chao et al., 2004). A simple model inspired by these findings is that OSM-9 is regulated by serotonin and acts downstream of MRCs to regulate both calcium transients in ASH and behavior. Such a role for serotonin is reminiscent of the proposed role for inflammation in behavioral responses to mechanical stimulation in mice (Miller et al., 2009).

The loss of *osm-9* can be complemented by transgenic expression of rat TRPV4 in ASH (Liedtke et al., 2003), suggesting that mammalian TRPV proteins may also act downstream of force detection in nociceptors and other sensory neurons. We note that this role for TRPV proteins in mechanosensation is fully compatible with their established role in temperature sensation in mammals (Caterina, 2007). TRPV channels expressed in mammalian nociceptors also respond to chemicals released as a consequence of tissue damage and inflammation and play critical roles in inflammation-induced peripheral sensitization (Basbaum et al., 2009; Smith and Lewin, 2009). We speculate that, because TRPV channels have pleiotropic roles in nociceptors, as primary detectors of temperature, as targets for inflammation-induced sensitization, and possibly as secondary signaling elements in mechanonociception, TRPV4 can substitute for OSM-9 as a secondary signaling component of mechanonociception in ASH.

Other TRP channels have been proposed to function downstream of MeT channels in mechanoreceptors. This role has been proposed for Painless in *Drosophila* multidendritic neurons (Zhong et al., 2010) and for both Nan and Iav in *Drosophila* hearing (Göpfert et al., 2006). Nan and Iav as well as the TRPN protein NompC are co-expressed in the chordotonal neurons that comprise the Johnston's organ (Gong et al., 2004; Kim et al., 2003; Lee et al., 2010; Liang et al., 2011). Chordotonal neurons fire action potential in response to sound and mediate a mechanical resonance of the *Drosophila* antennae that maximizes sound sensitivity. Both Iav and Nan are required for sound-evoked action potentials (Gong et al., 2004; Kim et al., 2003), but NompC is not (Eberl et al., 2000). However, loss of NompC eliminates mechanical resonance whereas loss of Iav and Nan lead to excessive antennal movements (Göpfert et al., 2006). Göpfert et al. (2006) argued that these data were consistent with NompC functioning as a MeT channel and that Nan and Iav might function to regulate NompC-dependent amplification. A working model emerging from our work and these studies is that TRP channels might function downstream of MeT channels to ensure that mechanosensory information is delivered to the central nervous system. The mechanism by which TRP channels provide this essential sensory function is not yet clear, but future work in ASH may provide an opportunity to investigate this question.

DEG/ENaC Channels Are Required for MRCs in Ciliated And Non-ciliated Neurons

A continuing mystery is exactly how mechanical loads are delivered to MeT channels in order to trigger channel opening *in vivo*. In ciliated mechanoreceptor neurons, the prevailing model is that mechanical stimulation may bend, compress, or extend the cilium lengthwise and that such movements that allow for channel activation by displacing protein tethers attached to the extracellular and intracellular surface of the MeT. This model implies that the machinery required to activate MeT channels localizes to the cilium. The identification here of DEG-1 and by others of TRP-4 (Kang et al., 2010) as essential pore-forming subunits of channels responsible for MRCs in ciliated neurons opens the door for structural tests of such tether-based models of MeT channel gating. The organization of non-ciliated mechanoreceptors is different and the mode of force dependent gating is also unknown. In

particular, MeT channel complexes localize to puncta that decorate the entire sensory dendrite of the non-ciliated *C. elegans* touch receptor neurons (Chelur et al., 2002; Cueva et al., 2007) and mechanical loads activate MeT channels by means of a local indentation (O'Hagan et al., 2005). The identification of DEG/ENaC-dependent mechanotransduction channels in ciliated (this study) and non-ciliated mechanoreceptors (O'Hagan et al., 2005) suggests that the mechanism of force transmission and force-dependent gating may be more similar in these morphologically distinct mechanoreceptor neurons than previously believed.

Experimental Procedures

Strains

Wild type animals were HA1134 *osm-10(rtIs27)* animals (gift from A. Hart, Brown University), an integrated, transgenic line expressing green fluorescent protein (GFP) under the control of an *osm-10* promoter. *rtIs27* was integrated into LG X from a stable line created by injecting *pha-1(e2123)* mutants with pHA#29 *Posm-10::GFP* (Faber et al., 2002) and pBX#1 to rescue the *pha-1* defect (Granato et al., 1994). HA1134 animals were out-crossed four times following integration and express GFP strongly in ASH, PHA, PHB, and weakly in ASI. With respect to avoidance of nose touch, HA1134 does not differ from the canonical wild-type strain, N2 Bristol (not shown).

The following mutant strains were used: HA1134 *pha-1(e2123) III;rtIs27* [*Posm-10::GFP; pha-1(+)*] X, GN132 *osm-9*(*ky10*) IV; *rtIs27* X, GN133 *ocr-2*(*ak47*) IV; *rtIs27* X, GN151 *deg-1*(*u443*)*rtIs27* X, GN152 *deg-1*(*u506u679*)*rtIs27* X, GN161 *unc-8*(*tm2071*) IV; *rtIs27* X, GN171 *osm-9*(*ky10*)*ocr-2*(*ak47*) IV; *rtIs27* X, GN194 *unc-8*(*tm2071*) IV; *deg1*(*u443*)*rtIs27* X, GN392 *osm-9(ky10)ocr-2(ak47) IV*; *deg-1(u443)rtIs27* X.

Behavioral Testing

Worms were tested for their ability to detect and avoid mechanical stimuli as young adults. They were synchronized and cultivated at 20°C for ~3 days using standard procedures. To test responses to nose touch, an eyelash hair was held in contact with the plate surface in front of moving worms; only events in which the worm's nose contacted the eyelash perpendicularly were scored. Each animal was subjected to 10 trials; a trial was considered positive if and only if contact with the eyelash elicited backward movement. All behavioral assays were conducted blind to genotype.

Assay plates were coated with a thin bacterial lawn prepared as follows. OP50-1 *E. coli* bacteria were prepared from an overnight culture and stored in 50mL aliquots at 4°C. Bacteria from an aliquot were pelleted and re-suspended in 5 mL of Luria Broth (LB); 200 µl was used to cover the surface of a 6 cm NGM plate. Plates were left open to dry 2 hours on the bench or 30 minutes under the chemical hood prior to behavioral assays. To prepare plates for drug assays, amiloride (300 µM) was added to the bacterial suspension before the plates were seeded. In addition, amiloride (300 µM) was added to plate medium (NMG) before they were poured and the plates were left to cool overnight before use.

in vivo Electrical Recording

Animals were immobilized using cyanoacrylate glue (QuickSeal, WPI, Sarasota, FL or WormGlu, Glustich, Delta, BC, Canada) and neuron cell bodies were exposed for whole-cell patch clamp recordings as described (Goodman et al., 1998). Briefly, internal hydrostatic pressure was released anterior to the vulva using a sharp glass dissection tool mounted on a hydraulic manipulator (Narishige MMO-203). ASH cell bodies were exposed by a small incision posterior to the nerve ring. We verified that the cell body and anterior axon remain

intact by viewing GFP fluorescence. Worms typically lived for more than an hour after gluing and dissection, as indicated by pharyngeal pumping and tail movement.

During dissection, mechanical stimulation and whole-cell patch clamp recordings, animals were mounted on the stage of an upright microscope (Nikon E600FN) equipped with Nomarski-DIC optics, epifluorescence, a 60x/1.0 NA water immersion objective and an analog CCD camera (Pulnix) connected to a VCR. Recording pipettes were pulled from borosilicate glass to a tip diameter of ~2 μm on a P-97 micropipette puller (Sutter Instruments) and shaped by pressure polishing (Goodman and Lockery, 2000). Pipettes had resistances of 5–15 MΩ when filled with normal internal saline that included 20 μM sulforhodamine 101 (Invitrogen). The whole-cell recording mode was achieved by a combination of suction and a brief voltage pulse ('zap'); success was verified by monitoring diffusion sulforhodamine-101 into the cell body.

Membrane current and voltage were amplified and acquired using an EPC-10 amplifier and Patchmaster software (HEKA Instruments). MRCs and MRPs were digitized at 5 kHz and filtered at 1 kHz. Responses to voltage ramps or series of voltage pulses were sampled at 5 kHz and filtered at 2 kHz. Recordings of membrane potential changes induced current injection were digitized at 10 kHz and filtered at 2 kHz. We also used the EPC-10 as a digital-to-analog converter to drive the piezoelectric bimorph used to deliver mechanical stimuli.

Control external saline was composed of (in mM): NaCl (145), KCl (5), $MgCl_2$ (5), $CaCl_2$ (1), HEPES (10), pH adjusted to 7.2 with NaOH. For sodium-free saline, an equimolar quantity of *N*-methyl-D-glucamine (NMG)-Cl was substituted for NaCl. The osmolarity of all external solutions was adjusted to ~325 mOsm with *D*-glucose (20 mM). Unless noted, internal solution contained (in mM): K-Gluconate (125), NaCl (22), $MgCl_2$ (1), $CaCl_2$ (0.6), Na-HEPES (10), K_2EGTA (10), pH adjusted to 7.2 with KOH. The osmolarity of internal solutions was ~315 mOsm. Amiloride (300 μM) was diluted from frozen stocks (1 mM in DMSO) into external saline immediately before each experiment. All chemicals were purchased from Sigma.

Data Analysis and Statistics

Electrophysiological data were analyzed using IgorPro v5–6 (Wavemetrics, Lake Oswego, OR). Input capacitance and series resistance were measured as described (Goodman et al., 1998). Recordings with series resistance greater than 76 MΩ were discarded. Voltage errors were corrected for liquid junction potentials, but not for small errors resulting from uncompensated series resistance. To obtain peak and steady-state current-voltage relationships of the net membrane current, we used the 'findpeaks' function (IgorPro) to measure peak current and averaged current recorded during the final 10 ms of each to compute steady-state values. Both peak and steady-state current were converted into current density based on measured input capacitance. As in O'Hagan et al. (2005), we used 'findpeaks' to measure peak MRCs and fit MRC waveforms with modified alpha functions to measure activation (τ_1) and decay (τ_2) time constants: $I(t) = G_{max}*(\exp(-t/\tau_2) - \exp(-t/\tau_1))*(V_h - E_{Na})$, where G_{max} is the estimated maximal conductance, V_h is the holding potential, and E_{Na} is the Nernst potential for Na+ ions in our solutions. Average values are reported as mean ± s.e.m. Statistical analyses were performed using IgorPro and InStat v3 (GraphPad Software Inc., La Jolla, CA).

Solution Exchange and Perfusion

Animals were continuously superperfused with normal external saline during all recordings. For most experiments, solution was delivered by a gravity-fed perfusion system and

removed using a peristaltic pump. For experiments involving the application of channel blocking drugs or ion substitution, we designed and fabricated a microfluidic chip to generate laminar flow in a 1-ml chamber under the water immersion objective. In this system, solutions were delivered with a peristaltic pump (flow rate: 2.4 ml per minute) and inflow was changed between control and experimental solutions *via* a manually controlled HPLC valve (Rheodyne, Rohnert Park, CA). Amiloride and Na^+-free saline were applied for at least one minute of continuous superfusion.

Delivery of Mechanical Stimuli

Controlled, mechanical stimuli were delivered using a calibrated glass probe whose movement was recorded on analog s-video tape during each experiment, as described (O'Hagan et al., 2005). The probe was moved using a piezoelectric bimorph (Piezo Inc, Boston, MA) driven by a custom-design, low-noise, high-voltage amplifier and controlled by voltage pulses delivered *via* the patch clamp amplifier (EPC-10), a buffer amplifier and filter (120 Hz) and control software (Patchmaster, HEKA, Bellmore, NY). Probes were fabricated from borosilicate glass rods (O.D. 1.2 mm) on a pipette puller (Sutter Instruments, Novato, CA) and mounted on the bimorph using beeswax to hold the probe inside a small glass sleeve.

Probe Calibration

In initial experiments, spring constants were measured by two independent methods. The first involved fabricating a set of known masses from a length of metal wire and measuring the displacement produced by hanging that mass from the tip of the probe. The effective spring constant, k, was found by fitting a plot of force ($=mg$) *vs*. displacement with a line. The second used a microelectromechanical system (MEMS) based force-sensor that was fabricated and calibrated (k = 12.9 N/m) as in (Park et al., 2007). The sensor was mounted on a piezoelectric actuator (PIHera P-622.Z; Physik Instrumente) and the tip of the sensor was brought into contact with the tip of the glass probe. The deflection of the glass probe for a given force was calculated from the difference between the movement of the piezoelectric actuator and the deflection of the force sensor. The spring constant of the glass probe was calculated from the measured force-displacement curves. The second method is more accurate and was used for all later probes. A total of 4 probes were used for this study, with spring constants between 22.2 and 43.3 N/m.

Analysis of Probe Movement and Calculation of Force Delivered

The probe tip was located and tracked in digitized video clips taken during stimulus application and free movement through saline. Tracking was accomplished either manually using NIH ImageJ as described (O'Hagan et al., 2005) or automatically using Visible™motion detection software (Reify Corporation, Saratoga, CA). Visible™locates moving objects such as our probe tip by generating instantaneous velocity vectors for each pixel of the image and associates a group of similar and adjacent motion vectors with the tip. Once the tip was successfully detected, the image region associated with the initial tip location was searched in each following frame to derive a measurement of the frame-by-frame movement of the probe tip. Image search was performed using Normalized Image Correlation. Thus, the distance that the tip moves at any time point is the euclidean distance between its location in the current and previous frames.

The distance moved by the probe tip *vs*. time was calculated for movements corresponding to the application of the probe to the worm's nose. The peak distance moved during load application (on nose), x_1, and during unloaded probe movement, x_2, in saline was computed from the average peak values in Matlab [MathWorks, Natick, MA]. The difference between these average distances gave the net deflection of the probe tip ($\Delta x = x_2 - x_1$). The force

applied was then computed by multiplying the respective spring constant (k) for the probe used and the net distance moved: $F = -k\Delta x$.

Measurement of Probe Resonant Frequency and Estimation of Probe Rise Time

To measure the resonant movement of the probes, we used a laser Doppler vibrometer (Polytec OFV3001) to measure the resonant frequency in air of stimulus probes mounted in the same configuration as they were for electrophysiological experiments. We estimated a resonant frequency in saline of 130 Hz and quality factor (Q) of ~7 from the measured resonant frequency in air (150 Hz) and the hydrodynamic function of an oscillating cylinder assuming laminar flow ($R_e \sim 8$) and an effective cylinder diameter of 100 microns (Rosenhead, 1963; Sader, 1998). We estimated the rise time to 90% of peak movement of the probe using the polynomial approximation given by: $T_r = (1.76\zeta^3 + 0.417\zeta^2 + 1.039\zeta+1)/\omega n$ using 130 Hz as the natural frequency (ω_n) and 0.5/Q as the dampening ratio (ζ) (Nise, 1998).

Supplementary Material

Refer to Web version on PubMed Central for supplementary material.

Acknowledgments

We thank C. Bargmann, M. Chalfie, A. Hart, M. Koelle, S. Mitani, the *C. elegans* Knockout Consortium, and the Caenorhabditis Genetic Center, which is funded by the NIH National Center for Research Resources (NCRR), for strains; Wormbase; T. Ozaki and A. Naim for help with initial data analysis; S. Husson, A. Gottschalk, S. Lechner, G. Lewin for sharing data prior to publication; and three anonymous reviewers. Work supported by NIH (NS047715, EB006745), the McKnight Foundation, the Donald B. and Delia E. Baxter Foundation, and fellowships from the Helen Hay Whitney Foundation (S.L.G.), the Swiss National Science Foundation (D.A.G.), NSF (J.C.D.), and the Stanford Medical School Dean's Fellowships (S.L.G., D.A.G.).

References

Arnadóttir J, Chalfie M. Eukaryotic mechanosensitive channels. Annu Rev Biophys. 2010; 39:111–137. [PubMed: 20192782]

Basbaum AI, Bautista DM, Scherrer G, Julius D. Cellular and molecular mechanisms of pain. Cell. 2009; 139:267–284. [PubMed: 19837031]

Bize V, Horisberger J-D. Sodium self-inhibition of human epithelial sodium channel: selectivity and affinity of the extracellular sodium sensing site. Am J Physiol Renal Physiol. 2007; 293:F1137–F1146. [PubMed: 17670907]

Caterina MJ. Transient receptor potential ion channels as participants in thermosensation and thermoregulation. Am. J Physiol Regul Integr Comp Physiol. 2007; 292:R64–R76. [PubMed: 16973931]

Chalfie M, Wolinsky E. The identification and suppression of inherited neurodegeneration in Caenorhabditis elegans. Nature. 1990; 345:410–416. [PubMed: 2342572]

Chao MY, Komatsu H, Fukuto HS, Dionne HM, Hart AC. Feeding status and serotonin rapidly and reversibly modulate a Caenorhabditis elegans chemosensory circuit. Proc Natl Acad Sci USA. 2004; 101:15512–15517. [PubMed: 15492222]

Chatzigeorgiou M, Schafer WR. Lateral Facilitation between Primary Mechanosensory Neurons Controls Nose Touch Perception in C. elegans. Neuron. 2011; 70:299–309. [PubMed: 21521615]

Chatzigeorgiou M, Yoo S, Watson JD, Lee W-H, Spencer WC, Kindt KS, Hwang SW, Miller DM, Treinin M, Driscoll M, Schafer WR. Specific roles for DEG/ENaC and TRP channels in touch and thermosensation in C. elegans nociceptors. Nat Neurosci. 2010; 13:861–868. [PubMed: 20512132]

Chelur DS, Ernstrom GG, Goodman MB, Yao CA, Chen L, O' Hagan R, Chalfie M. The mechanosensory protein MEC-6 is a subunit of the C. elegans touch-cell degenerin channel. Nature. 2002; 420:669–673. [PubMed: 12478294]

Chronis N, Zimmer M, Bargmann CI. Microfluidics for in vivo imaging of neuronal and behavioral activity in Caenorhabditis elegans. Nat Methods. 2007; 4:727–731. [PubMed: 17704783]

Colbert HA, Smith TL, Bargmann CI. OSM-9, a novel protein with structural similarity to channels, is required for olfaction, mechanosensation, and olfactory adaptation in Caenorhabditis elegans. J Neurosci. 1997; 17:8259–8269. [PubMed: 9334401]

Coste B, Mathur J, Schmidt M, Earley TJ, Ranade S, Petrus MJ, Dubin AE, Patapoutian A. Piezo1 and Piezo2 are essential components of distinct mechanically activated cation channels. Science. 2010; 330:55–60. [PubMed: 20813920]

Cueva JG, Mulholland A, Goodman MB. Nanoscale organization of the MEC-4 DEG/ENaC sensory mechanotransduction channel in Caenorhabditis elegans touch receptor neurons. J Neurosci. 2007; 27:14089–14098. [PubMed: 18094248]

Drew LJ, Wood JN, Cesare P. Distinct mechanosensitive properties of capsaicin-sensitive and -insensitive sensory neurons. J Neurosci. 2002; 22:RC228. [PubMed: 12045233]

Driscoll M, Chalfie M. The mec-4 gene is a member of a family of Caenorhabditis elegans genes that can mutate to induce neuronal degeneration. Nature. 1991; 349:588–593. [PubMed: 1672038]

Eberl DF, Hardy RW, Kernan MJ. Genetically similar transduction mechanisms for touch and hearing in Drosophila. J Neurosci. 2000; 20:5981–5988. [PubMed: 10934246]

Ezcurra M, Tanizawa Y, Swoboda P, Schafer WR. Food sensitizes C. elegans avoidance behaviours through acute dopamine signalling. EMBO J. 2011; 30:1110–1122. [PubMed: 21304491]

Faber PW, Voisine C, King DC, Bates EA, Hart AC. Glutamine/proline-rich PQE-1 proteins protect Caenorhabditis elegans neurons from huntingtin polyglutamine neurotoxicity. Proc Natl Acad Sci USA. 2002; 99:17131–17136. [PubMed: 12486229]

García-Añoveros J, Ma C, Chalfie M. Regulation of Caenorhabditis elegans degenerin proteins by a putative extracellular domain. Curr Biol. 1995; 5:441–448. [PubMed: 7627559]

Glauser DA, Chen WC, Agin R, MacInnis BL, Hellman AB, Garrity PA, Tan M-W, Goodman MB. Heat Avoidance is Regulated by Transient Receptor Potential (TRP) Channels and a Neuropeptide Signaling Pathway in Caenorhabditis elegans. Genetics. 2011; 188:91–103. [PubMed: 21368276]

Gong Z, Son W, Chung YD, Kim J, Shin DW, McClung CA, Lee Y, Lee HW, Chang D-J, Kaang B-K, et al. Two interdependent TRPV channel subunits, inactive and Nanchung, mediate hearing in Drosophila. J Neurosci. 2004; 24:9059–9066. [PubMed: 15483124]

Gonzales EB, Kawate T, Gouaux E. Pore architecture and ion sites in acid-sensing ion channels and P2X receptors. Nature. 2009; 460:599–604. [PubMed: 19641589]

Goodman MB, Hall DH, Avery L, Lockery SR. Active currents regulate sensitivity and dynamic range in C. elegans neurons. Neuron. 1998; 20:763–772. [PubMed: 9581767]

Goodman MB, Lockery SR. Pressure polishing: a method for re-shaping patch pipettes during fire polishing. J Neurosci Methods. 2000; 100:13–15. [PubMed: 11040361]

Goodman MB, Schwarz EM. Transducing touch in Caenorhabditis elegans. Annu Rev Physiol. 2003; 65:429–452. [PubMed: 12524464]

Göpfert MC, Albert JT, Nadrowski B, Kamikouchi A. Specification of auditory sensitivity by Drosophila TRP channels. Nat Neurosci. 2006; 9:999–1000. [PubMed: 16819519]

Granato M, Schnabel H, Schnabel R. pha-1, a selectable marker for gene transfer in C. elegans. Nucleic Acids Res. 1994; 22:1762–1763. [PubMed: 8202383]

Guo ZV, Hart AC, Ramanathan S. Optical interrogation of neural circuits in Caenorhabditis elegans. Nat Methods. 2009; 6:891–896. [PubMed: 19898486]

Hall DH, Gu G, García-Añoveros J, Gong L, Chalfie M, Driscoll M. Neuropathology of degenerative cell death in Caenorhabditis elegans. J Neurosci. 1997; 17:1033–1045. [PubMed: 8994058]

Hao J, Delmas P. Multiple desensitization mechanisms of mechanotransducer channels shape firing of mechanosensory neurons. J Neurosci. 2010; 30:13384–13395. [PubMed: 20926665]

Hardie RC. Phototransduction in Drosophila melanogaster. J Exp Biol. 2001; 204:3403–3409. [PubMed: 11707492]

Hart AC, Sims S, Kaplan JM. Synaptic code for sensory modalities revealed by C. elegans GLR-1 glutamate receptor. Nature. 1995; 378:82–85. [PubMed: 7477294]

Hilliard MA, Apicella AJ, Kerr R, Suzuki H, Bazzicalupo P, Schafer WR. In vivo imaging of C. elegans ASH neurons: cellular response and adaptation to chemical repellents. EMBO J. 2005; 24:63–72. [PubMed: 15577941]

Hu J, Lewin GR. Mechanosensitive currents in the neurites of cultured mouse sensory neurones. J Physiol (Lond). 2006; 577:815–828. [PubMed: 17038434]

Huang M, Chalfie M. Gene interactions affecting mechanosensory transduction in Caenorhabditis elegans. Nature. 1994; 367:467–470. [PubMed: 7509039]

Juusola M, Seyfarth EA, French AS. Sodium-dependent receptor current in a new mechanoreceptor preparation. J Neurophysiol. 1994; 72:3026–3028. [PubMed: 7897509]

Kang L, Gao J, Schafer WR, Xie Z, Xu XZS. C. elegans TRP Family Protein TRP-4 Is a Pore-Forming Subunit of a Native Mechanotransduction Channel. Neuron. 2010; 67:381–391. [PubMed: 20696377]

Kaplan JM, Horvitz HR. A dual mechanosensory and chemosensory neuron in Caenorhabditis elegans. Proc Natl Acad Sci USA. 1993; 90:2227–2231. [PubMed: 8460126]

Kim J, Chung YD, Park D-Y, Choi S, Shin DW, Soh H, Lee HW, Son W, Yim J, Park C-S, et al. A TRPV family ion channel required for hearing in Drosophila. Nature. 2003; 424:81–84. [PubMed: 12819662]

Kindt KS, Viswanath V, Macpherson L, Quast K, Hu H, Patapoutian A, Schafer WR. Caenorhabditis elegans TRPA-1 functions in mechanosensation. Nat Neurosci. 2007; 10:568–577. [PubMed: 17450139]

Lee J, Moon S, Cha Y, Chung YD. Drosophila TRPN(=NOMPC) channel localizes to the distal end of mechanosensory cilia. PLoS ONE. 2010; 5:e11012. [PubMed: 20543979]

Li W, Kang L, Piggott BJ, Feng Z, Xu XZS. The neural circuits and sensory channels mediating harsh touch sensation in Caenorhabditis elegans. Nat Commun. 2011; 2:315. [PubMed: 21587232]

Liang X, Madrid J, Saleh HS, Howard J. NOMPC, a member of the TRP channel family, localizes to the tubular body and distal cilium of Drosophila campaniform and chordotonal receptor cells. Cytoskeleton (Hoboken). 2011; 68:1–7. [PubMed: 21069788]

Liedtke W, Tobin DM, Bargmann CI, Friedman JM. Mammalian TRPV4 (VR-OAC) directs behavioral responses to osmotic and mechanical stimuli in Caenorhabditis elegans. Proc Natl Acad Sci USA. 2003; 100 Suppl 2:14531–14536. [PubMed: 14581619]

Lumpkin EA, Caterina MJ. Mechanisms of sensory transduction in the skin. Nature. 2007; 445:858–865. [PubMed: 17314972]

Lumpkin EA, Marshall KL, Nelson AM. The cell biology of touch. J Cell Biol. 2010; 191:237–248. [PubMed: 20956378]

McCarter GC, Reichling DB, Levine JD. Mechanical transduction by rat dorsal root ganglion neurons in vitro. Neurosci Lett. 1999; 273:179–182. [PubMed: 10515188]

Miller RJ, Jung H, Bhangoo SK, White FA. Cytokine and chemokine regulation of sensory neuron function. Handb Exp Pharmacol. 2009:417–449. [PubMed: 19655114]

Nise, N. Control Systems Engineering. Hoboken NJ: Wiley & Sons, Inc.; 1998.

O'Hagan, R. Components of mechanotransduction complex in *Caenorhabditis elegans* touch receptor neurons: an *in vivo* electrophysiological study. New York, NY: Colombia University; 2005. p. 135

O'Hagan R, Chalfie M, Goodman MB. The MEC-4 DEG/ENaC channel of Caenorhabditis elegans touch receptor neurons transduces mechanical signals. Nat Neurosci. 2005; 8:43–50. [PubMed: 15580270]

Park S-J, Goodman MB, Pruitt BL. Analysis of nematode mechanics by piezoresistive displacement clamp. Proc Natl Acad Sci USA. 2007; 104:17376–17381. [PubMed: 17962419]

Poole, K.; Lechner, SG.; Lewin, GR. The Molecular and Genetic Basis of Touch. In: Hertenstein, M.; Weiss, S., editors. The Handbook of Touch: Neuroscience, Behavioral, And Health Perspectives. New York, NY: Springer Publishing Co.; 2011. p. 59-84.

Perkins LA, Hedgecock EM, Thomson JN, Culotti JG. Mutant sensory cilia in the nematode Caenorhabditis elegans. Dev Biol. 1986; 117:456–487. [PubMed: 2428682]

Ramot D, MacInnis BL, Goodman MB. Bidirectional temperature-sensing by a single thermosensory neuron in C. elegans. Nat Neurosci. 2008; 11:908–915. [PubMed: 18660808]

Rosenhead, L. Laminar boundary layers; an account of the development, structure, and stability of laminar boundary layers in incompressible fluids, together with a description of the associated experimental techniques. Oxford Eng.: Clarendon Press; 1963.

Sader J. Frequency response of cantilever beams immersed in viscous fluids with applications to the atomic force microscope. J Appl Phys. 1998; 84:64–76.

Smith ESJ, Lewin GR. Nociceptors: a phylogenetic view. J Comp Physiol A Neuroethol Sens Neural Behav Physiol. 2009; 195:1089–1106. [PubMed: 19830434]

Tavernarakis N, Shreffler W, Wang S, Driscoll M. unc-8, a DEG/ENaC family member, encodes a subunit of a candidate mechanically gated channel that modulates C. elegans locomotion. Neuron. 1997; 18:107–119. [PubMed: 9010209]

Tobin D, Madsen D, Kahn-Kirby A, Peckol E, Moulder G, Barstead R, Maricq A, Bargmann C. Combinatorial expression of TRPV channel proteins defines their sensory functions and subcellular localization in C. elegans neurons. Neuron. 2002; 35:307–318. [PubMed: 12160748]

Tracey WD, Wilson RI, Laurent G, Benzer S. painless, a Drosophila gene essential for nociception. Cell. 2003; 113:261–273. [PubMed: 12705873]

Walker RG, Willingham AT, Zuker CS. A Drosophila mechanosensory transduction channel. Science. 2000; 287:2229–2234. [PubMed: 10744543]

Wang Y, Apicella A, Lee S-K, Ezcurra M, Slone RD, Goldmit M, Schafer WR, Shaham S, Driscoll M, Bianchi L. A glial DEG/ENaC channel functions with neuronal channel DEG-1 to mediate specific sensory functions in C. elegans. EMBO J. 2008; 27:2388–2399. [PubMed: 18701922]

Woolf CJ, Ma Q. Nociceptors--noxious stimulus detectors. Neuron. 2007; 55:353–364. [PubMed: 17678850]

Zhong L, Hwang RY, Tracey WD. Pickpocket Is a DEG/ENaC Protein Required for Mechanical Nociception in Drosophila Larvae. Curr Biol. 2010; 20:429–434. [PubMed: 20171104]

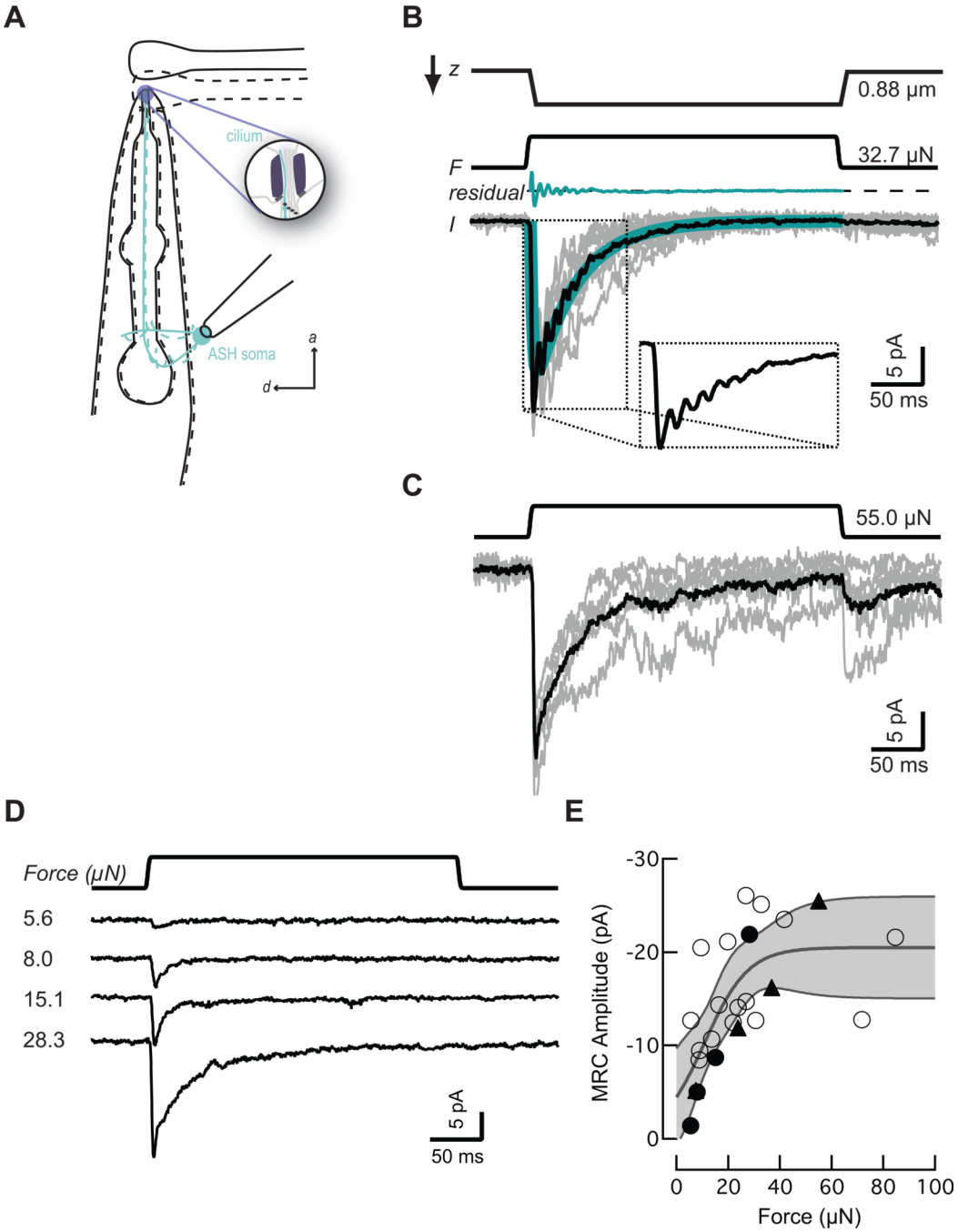

Figure 1. Mechanoreceptor Currents in ASH

(A) Schematic showing the geometry of force delivery to the nose during *in vivo* whole-cell patch-clamp recordings from ASH (aqua) in *C. elegans*. (B) Mechanoreceptor currents (MRCs) evoked in ASH by mechanical loads applied as shown in (A). The top two traces show probe displacement, *z*, and the force, *F*, applied. Below are MRCs evoked by ten stimuli (gray), their average (black), a fit to the data with an alpha function (aqua, thick), and the residuals between the average and the fit (aqua, thin). Probe movement triggered resonant oscillations of the probe tip, which evoked sinusoidal variations in current (inset). Oscillation frequency was 122 Hz (aqua, thin). (C) MRCs in ASH showing both ‘on’ and ‘off’ responses. Shown are responses to five stimuli (gray) and their average (black). (D)

MRC amplitude increased with force. Similar results were obtained in a total of five recordings. (E) Force-dependence of MRCs. Collected results from individual ASH neurons challenged with force pulses of a single amplitude (open circles) or a series of force pulses covering a range of amplitudes (filled circles, triangles). The solid line is a fit to the data with a Boltzmann function whose parameters are −20 pA, 11 μN, and 8 μN for the maximum amplitude, half-maximal force, and slope factor. Shaded area indicates the 95% confidence bands for the fit.

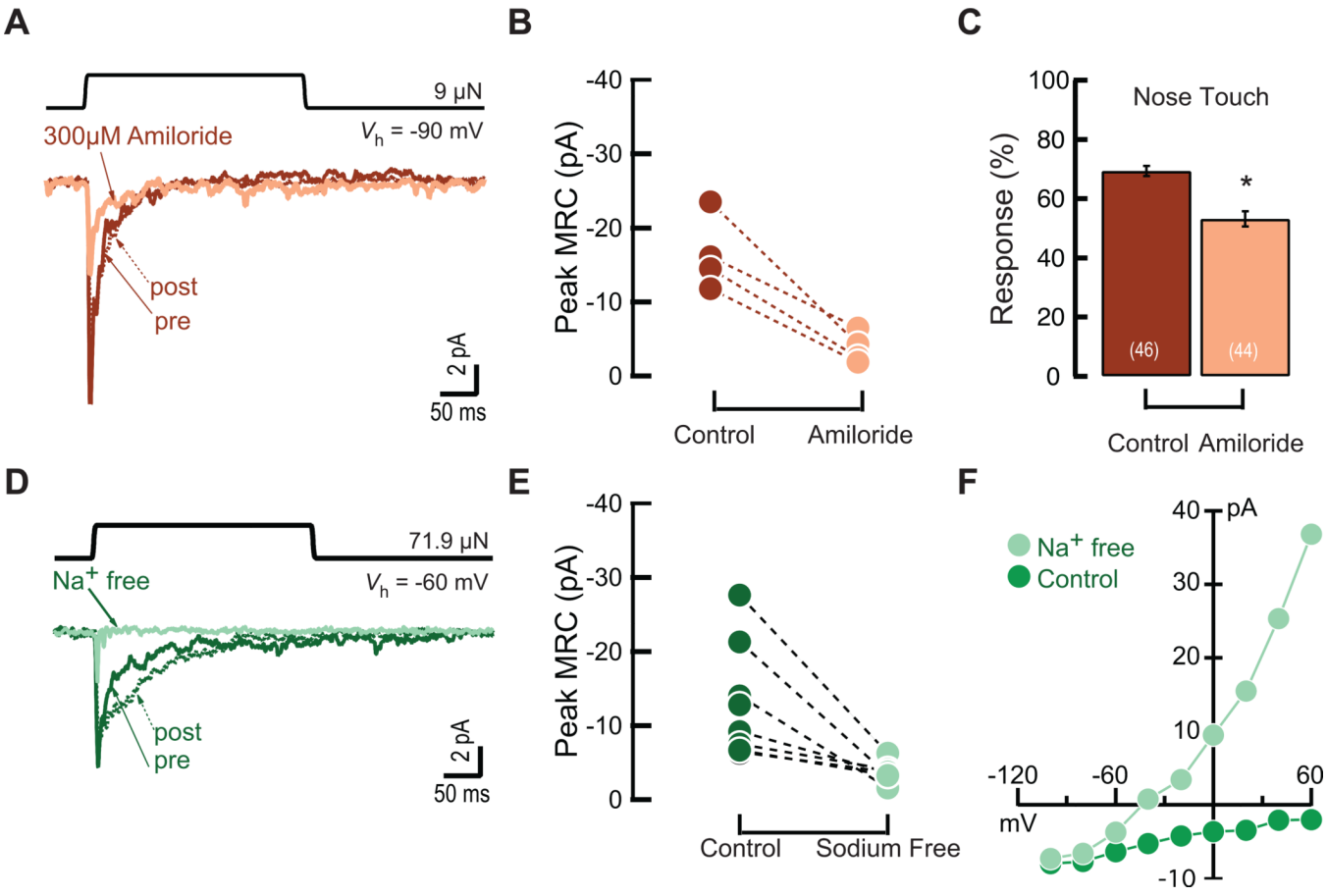

Figure 2. MRCs Were Reduced in Amiloride and in Na^+-free External Saline

(A, B) MRCs in wild-type ASH neurons were decreased by amiloride. Holding potential: −90 mV. The three traces were recorded before (pre), during (300µM amiloride), after (post) superfusion with amiloride. (C) Nose touch responses of worms were reduced by 300 µM amiloride. *$p < 0.001$ Mann-Whitney rank test. (D, E) Inward MRCs were decreased in Na^+-free saline. Holding potential: −60 mV. The three traces were recorded before (pre), during (Na^+-free), and after superfusion (post) of Na^+-free saline. (F) Peak MRC amplitude *vs.* voltage in control (dark green) and Na^+-free (light green) saline recorded from the same cell as in panel D.

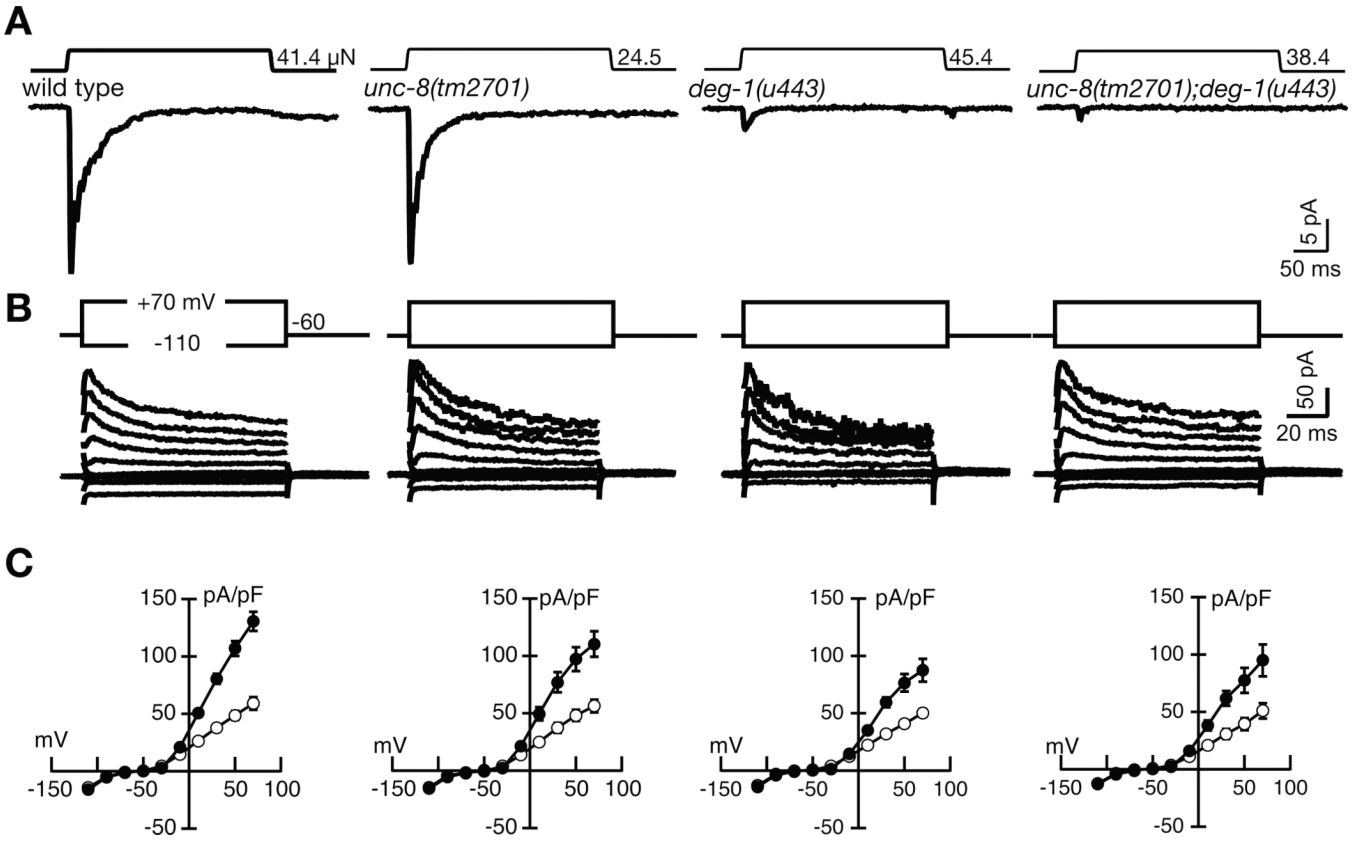

Figure 3. Loss of *deg-1*, but not *unc-8* Decreases MRCs

(A) MRCs in wild-type, *unc-8(tm2701)* and *deg-1(u443)* single null mutants and *unc-8;deg-1* double null mutants. Stimuli were >20µN for all genotypes. Holding potential: −60 mV. (B) Voltage-activated net membrane current in the same cells as in A. (C) Average current-voltage (*I–V*) relationships for all four genotypes ($n \geq 4$) showing peak current (filled) and steady-state (open) current during 100 ms voltage pulses.

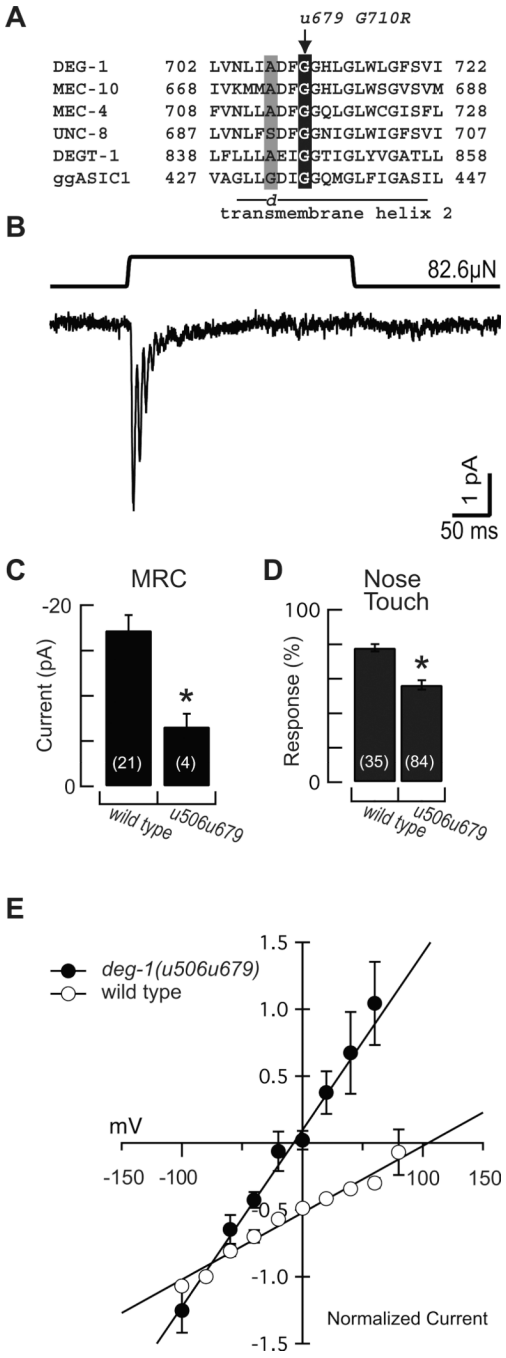

Figure 4. Missense Mutations in *deg-1* Alter MRC Selectivity

(A) Sequence alignment of selected *C. elegans* DEG/ENaC proteins and *Gallus gallus* ASIC1a. The second transmembrane domain was identified based on the high-resolution structure available for the ggASIC1a protein (Gonzales et al., 2009). To provide a common reference frame across DEG/ENaC family members, the degeneration or *d* position is indicated in gray. Mutating this residue in DEG-1, MEC-4, or MEC-10 causes degeneration *in vivo* (Chalfie and Wolinsky, 1990; Driscoll and Chalfie, 1991; Huang and Chalfie, 1994). Mutating a conserved glycine, highlighted in black) in MEC-4 and MEC-10 alters selectivity *in vivo* (O'Hagan et al., 2005). (B, C) *deg-1(u506u679)* mutants retained MRCs with decreased amplitude. Holding potential = −60 mV. **p* = 0.0009, two-tailed *t* test. (D) Nose

touch responses are reduced in *deg-1(u506u679)* mutants. *$p < 0.0001$ Mann-Whitney rank test. (E) *I–V* relationship of MRCs in wild type (open, $n \geq 3$) and *u506u679* mutants (filled, $n = 4$). Current was normalized to the value measured at −80mV in each recording. The solid lines were fit to the MRC *I–V* relationship in wild type and *u506u679* mutant ASH neurons.

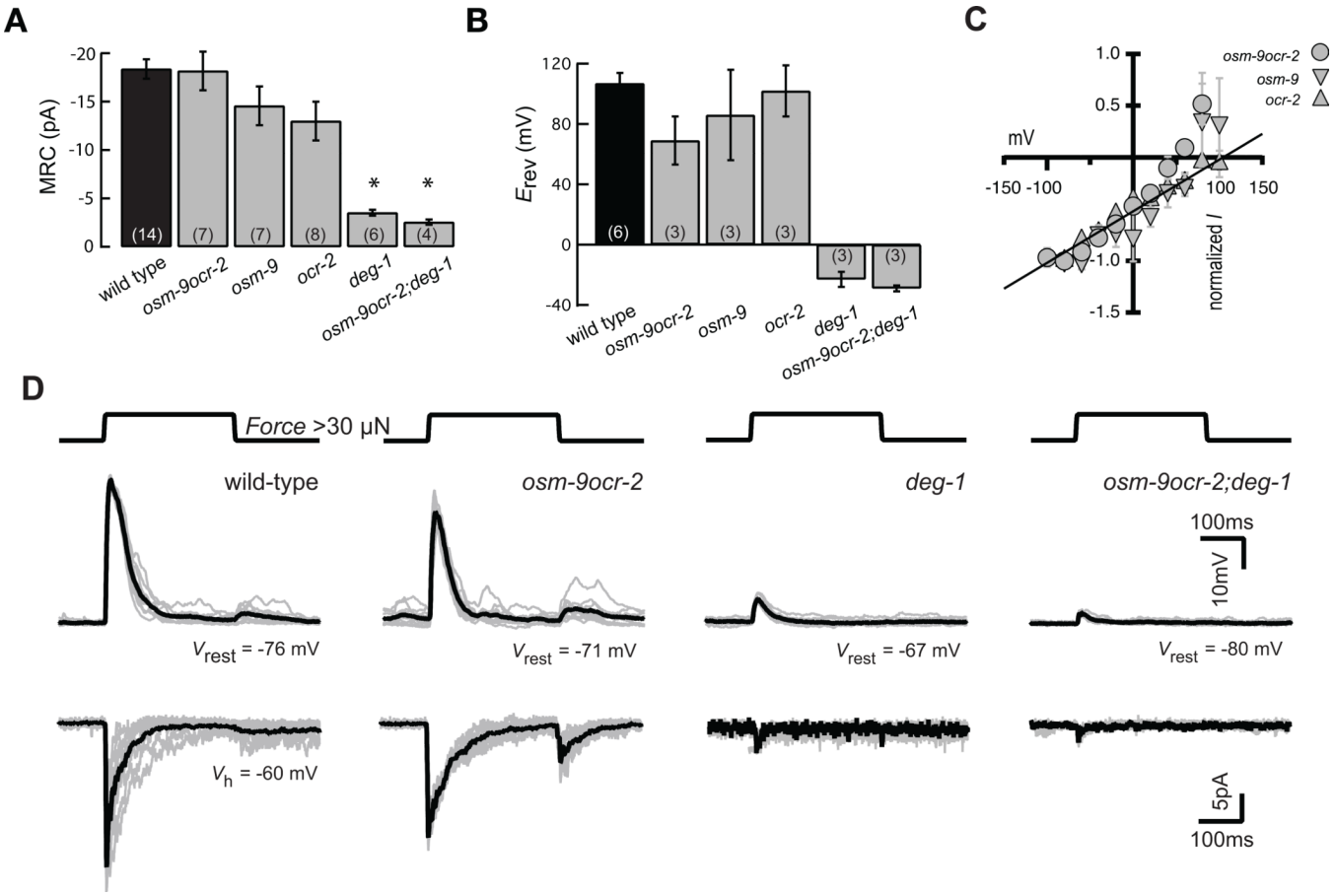

Figure 5. Electrical Responses to Force Are Intact in *ocr-2, osm-9,* and *osm-9ocr-2* Mutants, but Disrupted in *deg-1* Mutants

(A) Average peak MRCs in wild-type and null mutant ASH neurons. Holding potential: −60 mV. *Values significantly different than wild type, $p < 0.05$ (one-way ANOVA $F_{8, 54}= 9.4$, $p<0.0001$, Tukey-Kramer multiple comparisons test). (B) Average reversal potential of peak MRCs in wildtype and mutant ASH neurons. (C) *I–V* relationship of MRCs in mutant ASH neurons normalized to the value measured at −80 mV. Solid line is reprinted from Figure 4E and shows the fitted relationship for wild type MRCs. (D) MRPs (middle) and MRCs (bottom) from wild type, *osm-9ocr-2* double null mutant, *deg-1* null mutant and *osm-9ocr-2;deg-1* triple null mutant ASH neurons. Individual responses to ten stimuli are shown in gray and their average is shown in black. Stimuli were >30µN for all genotypes.

Table 1

	n	Peak MRC (pA)	Latency (ms)	τ_1 (ms)	τ_2 (ms)	Average Force (μN)	Force Range (min-max, μN)
wild type	*14*	−18 ± 1	3.4 ± 0.1	1.9 ± 0.1	33 ± 5	38 ± 5	22–85
unc-8;deg-1	*7*	−3.1 ± 0.5 *	4.4 ± 0.5	3.3 ± 0.7 *	14 ± 5	35 ± 4	25–56
unc-8	*6*	−18 ± 5	2.8 ± 0.1	1.9 ± 0.1	59 ± 25	47 ± 16	25–125
deg-1	*6*	−3.5 ± 0.3 *	3.6 ± 0.2	3.0 ± 0.6	9 ± 1	42 ± 5	31–66
deg-1(u506u679)	*4*	−7 ± 1 *	3.4 ± 0.3	2.0 ± 0.3	45 ± 34	51 ± 11	30–83
osm-9ocr-2	*7*	−18 ± 2	3.1 ± 0.3	2.6 ± 0.4	31 ± 7	35 ± 3	24–46
osm-9	*7*	−15 ± 2	3.7 ± 0.3	2.6 ± 0.3	34 ± 6	35 ± 3	23–45
ocr-2	*8*	−13 ± 2	3.7 ± 0.3	2.5 ± 0.2	39 ± 10	38 ± 6	23–78
osm-9ocr-2; *deg-1*	*4*	−2.5 ± 0.3 *	6.2 ± 2.1 *	1.8 ± 0.4	16 ± 5	43 ± 10	26–74

Values are mean ± s.e.m., except where indicated. Alleles are null unless noted.

* Values significantly different than wild type, one-way ANOVA and Tukey-Kramer multiple comparisons test: Peak MRCs (ANOVA $F_{8, 54}$= 9.5, p<0.0001, *post-hoc test p<0.05); Latency (ANOVA $F_{8, 54}$= 2.9, p=0.0084, *post-hoc test p<0.01); τ_1 (ANOVA $F_{8, 54}$= 2.3, p=0.0357, *post-hoc test p<0.05); τ_2 (ANOVA $F_{8, 54}$= 1.7, p=0.1); Force (ANOVA $F_{8, 54}$= 0.5, p=0.9).

Table 2

	n	V_m (mV)	Peak MRP (mV)	ΔV (mV)	Force (μN)	Force Range (min-max, μN)
wild type	*10*	−67 ± 2	−39 ± 3	28 ± 3	52 ± 6	20–48
unc-8;deg-1	*3*	−61 ± 5	−56 ± 3 *	5 ± 2 *	37 ± 5	31–46
deg-1	*3*	−71 ± 3	−66 ± 3 *	8 ± 2 *	38 ± 6	31–49
osm-9ocr-2	*5*	−69 ± 3	−35 ±2	34 ± 3	50 ± 8	29–41
osm-9ocr-2;deg-1	3	−78 ± 2 *	−74 ± 4 *	4 ± 2 *	49 ± 7	35–58

Values are mean ± s.e.m., except where indicated. Forces applied to mutants were not significantly different than those applied to wild type, Mann-Whitney rank test.

* Values significantly different than wild type, Mann-Whitney rank test: Peak MRPs ($p<0.05$); V_m ($p<0.05$); ΔV ($p<0.01$).